

## Carbon in silicon: Modeling of diffusion and clustering mechanisms

R. Pinacho,<sup>a)</sup> P. Castrillo, M. Jaraiz, I. Martin-Bragado, and J. Barbolla

*Department of Electronics, University of Valladolid, Campus Miguel Delibes, 47011 Valladolid, Spain*

H.-J. Gossmann, G.-H. Gilmer,<sup>b)</sup> and J.-L. Benton

*Agere Systems, Murray Hill, New Jersey 07974*

(Received 13 March 2002; accepted for publication 9 May 2002)

Carbon often appears in Si in concentrations above its solubility. In this article, we propose a comprehensive model that, taking diffusion and clustering into account, is able to reproduce a variety of experimental results. Simulations have been performed by implementing this model in a Monte-Carlo atomistic simulator. The initial path for clustering included in the model is consistent with experimental observations regarding the formation and dissolution of substitutional C–interstitial C pairs ( $C_s-C_i$ ). In addition, carbon diffusion profiles at 850 and 900 °C in carbon-doping superlattice structures are well reproduced. Finally, under conditions of thermal generation of intrinsic point defects, the weak temperature dependence of the Si interstitial undersaturation and the vacancy supersaturation in carbon-rich regions also agree with experimental measurements. © 2002 American Institute of Physics. [DOI: 10.1063/1.1489715]

### INTRODUCTION

Carbon is present in silicon as a substitutionally dissolved isovalent impurity, introduced during crystal growth. It appears in high concentrations, ranging from  $10^{15} \text{ cm}^{-3}$  to  $10^{18} \text{ cm}^{-3}$ , well above its solubility at the usual annealing temperatures. Recently, the study of carbon kinetics in silicon has aroused a great interest because it has been proven to be an effective trap for Si self-interstitials (I). The presence of high carbon concentrations ( $\geq 10^{19} \text{ cm}^{-3}$ ) leads to an I undersaturation which, in turn, reduces boron diffusion.<sup>1</sup> Consistent with this, there is experimental evidence that carbon can reduce the implantation-induced I supersaturation and thus prevent the transient enhanced diffusion of interstitially diffusing dopants such as boron.<sup>2</sup>

The mechanism that controls carbon diffusion and, at the same time, accounts for the trapping of I is widely assumed to be the kick-out mechanism ( $C_s + I \leftrightarrow C_i$ ).<sup>3</sup>  $C_s$  denotes a carbon in a substitutional position that can be considered immobile while  $C_i$  is the highly mobile species that is either a carbon in an interstitial position, or a pair of a substitutional carbon and a self-interstitial. With this simple model, and using for the kick-out mechanism the activation energy extracted from well-established experiments of silicon self-diffusion<sup>4</sup> and of carbon solubility and in-diffusion<sup>5,6</sup> in addition to measurements of the diffusivity of  $C_i$ ,<sup>3</sup> the experiments cannot be reproduced satisfactorily. Some of the points that remain unclear are the following: (i) The experiments exhibit a diffusion that is faster than that predicted by the simple kick-out model,<sup>7</sup> (ii) the measured self-interstitial undersaturation produced by carbon under thermal intrinsic point defect generation conditions is independent of temperature,<sup>1</sup> in contrast with the predictions of the model,

(iii) a vacancy (V) supersaturation has been experimentally observed in regions with a high carbon concentration ( $10^{20} \text{ cm}^{-3}$ ) and it cannot be generated assuming the kick-out mechanism alone,<sup>8</sup> and (iv) the  $C_s-C_i$  pairing is not usually included in the carbon diffusion models, although it is a well established fact.<sup>9</sup> Therefore, a more comprehensive model is needed that can account not only for the diffusion of carbon but also for its initial stages of clustering.

Some modifications have been added to the kick-out model in order to explain the above mentioned experimental facts. Recently, Scholz *et al.*<sup>10</sup> suggested that an accurate description of the experimental profiles is only possible if the Frank–Turnbull mechanism ( $C_s \leftrightarrow C_i + V$ ) is additionally taken into account. At high concentrations of substitutional carbon the forward reaction would be likely to happen and would explain both the enhanced carbon diffusion (higher concentration of mobile  $C_i$ ) and the observed V supersaturation. However, the activation energy for the forward reaction of the Frank–Turnbull mechanism to be relevant at the experimental temperatures implies a very low V formation energy, that was estimated to be about 2.2 eV. Although this value was interpreted in a manner consistent with the formation energy extracted from some diffusion experiments,<sup>11</sup> it is in contrast with the values obtained from first-principles calculations, that range between 3.3 eV<sup>12</sup> and 4.1 eV.<sup>13</sup> The apparent low value (around 2 eV) extracted from diffusion experiments could be explained by V trapping, perhaps the vacancy–oxygen pair (VO) that has a binding energy of about 1.7 eV.<sup>10,12</sup> The formation of the VO pair conveys the trapping of vacancies, thus altering the extracted V formation energy. Then, these experiments would only yield an *effective* V formation energy. Consequently, the activation energy of the Frank–Turnbull mechanism cannot be extracted from it.

On the other hand, the above-mentioned model does not take into account the fact that, as carbon is above its solubility limit at the annealing temperatures, a thermodynamic

<sup>a)</sup>Electronic mail: ruth@ele.uva.es

<sup>b)</sup>Permanent address: Lawrence Livermore National Laboratory, P.O. 808, Livermore, CA 94551

driving force will exist for a precipitation process. This precipitation process should in the end lead to the formation of silicon carbide (SiC), provided the interface and stress energies (or an insufficient diffusivity at low temperatures) do not prevent precipitation. Since the SiC–Si interface energy is extremely high,<sup>3</sup> carbon precipitation in Si is generally an unlikely process even in the presence of a high carbon supersaturation. As an alternative to SiC formation a simple agglomeration of carbon atoms can be considered.<sup>3</sup> Therefore, parallel to the diffusion of carbon, an increasing number of immobile carbon/self-interstitial (C/I) clusters are formed. Clustering is a diffusion-assisted process and can lead to a change in the effective diffusivity of carbon, as it has been previously shown.<sup>14</sup>

In this work, a comprehensive model to explain the carbon behavior under thermal intrinsic point defects generation conditions is presented. In addition to the kick-out and Frank–Turnbull mechanisms for carbon diffusion, C/I cluster formation/dissolution mechanisms are also included. As it turns out, this model explains well the carbon diffusion behavior as well as the independence of I undersaturation of temperature. At the same time, it correctly predicts the existence of a V supersaturation using a V formation energy consistent with positron annihilation experiments and with first-principles calculations. Also, the formation of C/I clusters yields an immobile fraction of carbon in the carbon rich-regions that could act as seeds for precipitation. Finally, the initial path for clustering is consistent with the  $C_s$ – $C_i$  pairing experiments at low temperature. In order to test the accuracy of the model, we have implemented it into the kinetic Monte-Carlo simulator DADOS.<sup>15</sup> This simulator is able to incorporate both diffusion and complex clustering paths simultaneously with almost no computation time increase.

## THE MODEL

Similar to the previous models developed by other authors, the model presented here is based on the kick-out and Frank–Turnbull mechanisms for carbon diffusion, and  $C_i$  is assumed to be the only mobile carbon species. The reactions are:



Table I summarizes the prefactor and energy values that we assume for the diffusivities and the equilibrium concentrations of I and V, as well as for the  $C_i$  diffusivity. Diffusivities and concentrations relate to the general form  $D_X = D_0 \exp(-E_m/kT)$  and  $[X]^* = [X]_0^* \exp(-E_f/kT)$ , where  $E_m$  and  $E_f$  are the migration and formation energies, respectively. The products  $D_I \cdot [I]^*$  and  $D_V \cdot [V]^*$  correspond to the well-established values from Ref. 4. The migration energy of  $C_i$  is taken from Ref. 16. The values of  $D_{C_i}$  and  $D_I$  at low temperature resulting from the parameters of Table I are in good agreement with the values measured in Refs. 3 and 17, respectively. Note, in particular, that the V formation energy ( $E_{fV}$ ) has a value of 3.7 eV, consistent with *ab-initio* calculations.<sup>12,13</sup>

TABLE I. Simulation parameters.  $D_I$ ,  $D_V$ , and  $D_{C_i}$  are the I, V and  $C_i$  diffusivities, respectively.  $[I]^*$  and  $[V]^*$  are I and V equilibrium concentrations. The binding energy of  $C_i$  is assumed to be 1.5 eV according to Ref. 18. Note that  $E_{\text{Diff,C}} = E_{mC_i} + E_{fI} - E_{bC_i} = 3.23$  eV, consistent with the experiments in Ref. 5.

Parameter	$D_0, [X]_0^*$	$E_m, E_f$ (eV)
$D_I$	2 cm <sup>2</sup> /s	0.9
$[I]^*$	$1.45 \times 10^{25}$ cm <sup>-3</sup>	4
$D_V$	$1 \times 10^{-3}$ cm <sup>2</sup> /s	0.44
$[V]^*$	$4.6 \times 10^{25}$ cm <sup>-3</sup>	3.7
$D_{C_i}$	$1 \times 10^{-3}$ cm <sup>2</sup> /s	0.73

The backward reaction in reaction 1 involves the binding energy of  $C_i$  ( $E_{bC_i}$ ) that is assumed to be 1.5 eV, according to Ref. 18. These values imply an activation energy for carbon diffusion of  $E_{\text{Diff,C}} = E_{mC_i} + E_{fI} - E_{bC_i} = 3.23$  eV, not far from the values measured in Ref. 5 (3.04 eV). It is worthy to point out that with this set of energies, the dissociative mechanism (Frank–Turnbull) ( $C_s \rightarrow V + C_i$ ) has a high activation energy ( $E_{F-T} = E_{fV} + E_{fI} - E_{bC_i} + E_{mV} = 6.64$  eV) and is not dominant at the annealing temperatures.

In our model, higher order interactions involving  $C_s$ ,  $C_i$ , I, and V have been considered to simulate the growth and dissolution of immobile clusters. A cluster of  $n$  carbon atoms, having a total of  $m$  atoms (either carbon or silicon) at interstitial positions will be denoted as  $C_n I_m$ . We will assume that all the possible microscopic configurations of a given pair ( $n, m$ ) are equivalent (or can be represented by an effective parameter set).

The first steps of this clustering process are summarized in the following lines: as  $C_i$  migrates, it is likely to meet a  $C_s$  along its path, specially in regions of a high carbon content, and form the  $C_s$ – $C_i$  immobile pair,<sup>9–19</sup> that will be represented as  $C_2 I$  cluster in our notation. The reaction is described by



The binding energy of  $C_i$  in the  $C_2 I$  cluster involved in this reaction has been recently calculated as  $E_{bC_i}^{C_2 I} = 0.8$  eV.<sup>18</sup>

In addition, the  $C_2 I$  cluster can break up either by emitting a  $C_i$  (Reaction 3) or by the emission of an I leaving an immobile  $C_2$  cluster:



These small clusters can grow by trapping either I or  $C_i$  that are rapidly diffusing across the material. Similarly to the case of boron clustering,<sup>20</sup> the reaction paths for the growth of  $C_n I_m$  clusters can be visualized on a two-dimensional array, as shown in Fig. 1. The reactions that govern the growth/dissolution of these clusters are:



(trapping/emission of a  $C_i$ ),



(trapping/emission of an I).

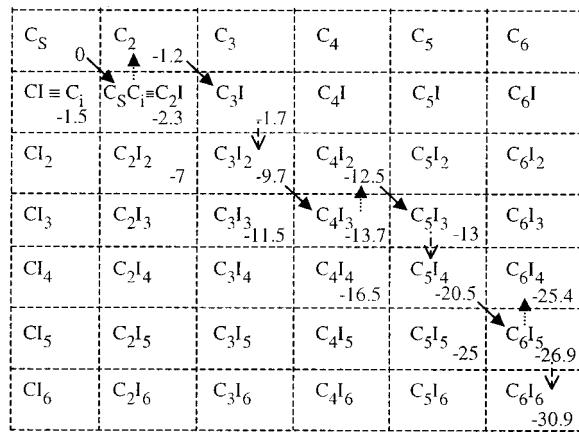


FIG. 1. Potential energy map (in eV) of  $C_nI_m$  clusters and schematic of the path for their growth under conditions of intrinsic point-defects thermal generation. Solid lines correspond to forward reaction 5, dotted lines to backward reaction 6, and dashed lines to forward reaction 7. The clusters  $C_nI_m$  whose potential energy have not been indicated are supposed to be much more unstable (high potential energy) so they do not appear in the simulated conditions.

As it can be seen, the forward reactions lead to the growth of the clusters and are diffusion-assisted. Therefore the path for the growth of carbon/self-interstitial clusters strongly depends on the initial intrinsic point defects conditions and type of annealing (inert or oxidizing atmosphere).

In addition, there is a third mechanism for cluster growth included in the simulations that, in contrast to the previous ones, is not diffusion-assisted. The  $C_nI_m$  clusters can trap a neighbor silicon atom placed in the lattice and release a V:



(trapping/emission of a V).

Note that the emission of a V from a  $C_nI_m$  cluster is the natural reverse reaction of the trapping of a V by the clusters and its subsequent annihilation with an I. This reaction creates a V that diffuses away. It can be thought of as the equivalent of the Frank–Turnbull mechanism but in this case for the C/I clusters instead of  $C_s$  (reaction 2).

Figure 2 shows the energy diagram for cluster growth with reactions (6) and (7). As it can be seen, these two reactions represent competing processes and the former would be favored under high I flux conditions. On the other hand, according to Fig. 1, the activation energy for a  $C_nI_m$  cluster (reaction 7) to emit a V and form the cluster  $C_nI_{m+1}$  is:

$$E_{act,V}^{C_nI_m} = E_f^I + E_f^V - E_{bl}^{C_nI_{m+1}} + E_m^V, \quad (8)$$

where  $E_{bl}^{C_nI_{m+1}}$  is the binding energy of an I to a cluster  $C_nI_{m+1}$ , defined as the difference between the potential energy of the  $C_nI_m$  and  $C_nI_{m+1}$  clusters. As the formation energies of vacancies and self-interstitials have a high value (Table I), reaction (8) would be relevant only if  $E_{bl}^{C_nI_{m+1}}$  is high enough. This will happen when the potential energy of  $C_nI_{m+1}$  is much lower than the potential energy of  $C_nI_m$ .

The best energy set for the C/I clusters that we obtain by fitting the available experimental data is given in the schematic of Fig. 1. Entropy changes due to differences in the atomic vibrational amplitudes of different defects are ne-

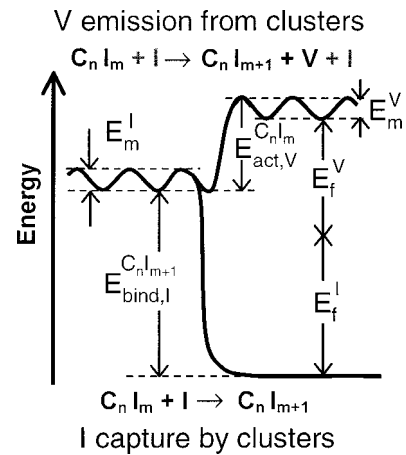


FIG. 2. Potential energy diagram of two of the competing processes (reactions 6 and 7) that give origin to carbon clustering. An I has been added to reaction 7 (top) in order to start from the same initial configuration energy as for reaction 6.

glected. This implies that the prefactors used in the emission of the different particles from the clusters are taken to be  $6D_0/\lambda^2$ ,  $D_0$  being the diffusion prefactor of the emitted species and  $\lambda$  the jump distance.

Some comments about the stability of C/I clusters can be found in the literature.<sup>3</sup> It is thought that, as carbon is smaller than silicon, carbon agglomeration can lead to a local volume contraction of about one atomic volume per each carbon atom incorporated. Therefore, growth of carbon agglomerates without excessive stress and plastic deformation can proceed only if for every carbon atom incorporated a self-interstitial is absorbed, or alternatively a V is emitted. Then, the energies of the C/I clusters with the same content of carbon and self-interstitial ( $C_nI_n$ ) are much lower than for any other composition, leading, for high temperatures and/or long times, to the formation of big C/I clusters with  $C_nI_n$  stoichiometry. However, the initial agglomerate stages, that is, the small carbon clusters, are suggested to have about 10%–15% less volume per carbon atom than SiC.<sup>21</sup> This means that for small sizes, the more stable  $C_nI_m$  clusters are those with a slightly lower content of I than C ( $C_3I_2, C_4I_2, \dots$ ) in agreement with the energy map of Fig. 2.

## RESULTS

### $C_s-C_i$ formation and breakup at low temperatures

The first steps of C/I clustering formation can be compared with recent experimental results at low temperatures.<sup>19</sup> In those experiments, carbon-rich silicon was irradiated with electrons at cryogenic temperatures and subsequently heated to room temperature and analyzed by infrared absorption spectroscopy (IRS). Electron irradiation generates intrinsic point defects and  $C_i$  is formed as the temperature is raised, as revealed by the presence of  $C_i$ -related absorption peaks. At room temperature,  $C_i$  is mobile and is trapped by the background carbon, giving rise to the formation of  $C_s-C_i$  pairs ( $C_2I$  in our cluster notation), following reaction (3). Figure 3(a) shows the time evolution of the  $C_s-C_i$  concentration formed at room temperature, as inferred from IRS

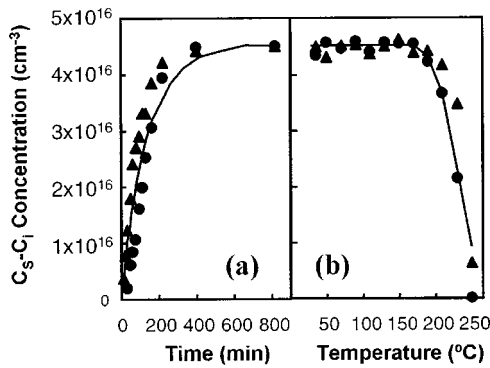


FIG. 3. Concentration of  $C_s-C_i$  ( $C_2I$  in our cluster notation) in electron-irradiated carbon-doped silicon (a) as a function of the time that the sample is maintained at room temperature and (b) after each step of a series of isochronal (30 min) heat treatments. The total carbon concentration is  $4.5 \times 10^{17} \text{ cm}^{-3}$ . The experimental data (symbols) are inferred from the intensities of the two strongest absorption lines [ $7819 \text{ cm}^{-1}$  ( $\blacktriangle$ ) and  $730 \text{ cm}^{-1}$  ( $\bullet$ )] (Ref. 20). Simulated concentrations (lines) have been obtained assuming an initial  $C_i$  concentration of  $6 \times 10^{16} \text{ cm}^{-3}$  and a room temperature of 300 K.

intensities.<sup>19</sup> If the samples are subsequently annealed at higher temperatures, of the order of 200 °C,  $C_s-C_i$ -related IRS intensities decrease and, eventually disappear. This behavior is displayed in Fig. 3(b).<sup>19</sup>

We have simulated the formation and breakup of  $C_s-C_i$  using the model and parameters described in the previous section. The two nonequivalent configurations (A and B) of  $C_s-C_i$  pairs<sup>19</sup> have been represented in our model by one effective configuration that we have denoted by  $C_2I$  cluster. To account for the electron irradiation generated  $C_i$  we assume an initial uniform distribution of  $C_i$  on the  $C_s$  background, with a total carbon concentration equal to the value estimated by IRS ( $4.5 \times 10^{17} \text{ cm}^{-3}$ ). At room temperature  $C_i$  can migrate and form  $C_2I$  and, in a lower proportion,  $C_2I_2$  and  $C_3I_2$  clusters, formed through the forward Reaction 5. Since the initial  $C_i$  concentration is not given in Ref. 19, we have set its value to  $6 \times 10^{16} \text{ cm}^{-3}$  so that the final  $C_2I$  concentration at room temperature best fits the experimental es-

timate. The simulated evolution of  $C_2I$  concentration is included in Fig. 3(a). Subsequent heating steps at higher temperatures induce the thermal breakup of  $C_2I$ , in good agreement with the experimental results [Fig. 3(b)]. In our simulations this breakup occurs mainly through the emission of  $C_i$  ( $C_2I \rightarrow C_s + C_i$ ) that can be captured by another more stable cluster ( $C_i + C_2I \rightarrow C_3I_2$ ) giving rise to cluster growth. The other possible breakup process ( $C_2I \rightarrow C_2 + I$ ) is found to be less frequent in the conditions of Fig. 3(b).

### Carbon diffusion experiments at annealing temperatures

In order to test the accuracy of the new model at annealing temperatures, we compared experimental diffused secondary ion-mass spectroscopy (SIMS) profiles of carbon with those simulated with DADOS. In this case, we also monitored the simulated time-averaged concentrations of intrinsic point defects, because they can be directly compared with experimental self-interstitial undersaturation reported in the literature.<sup>2</sup> We utilized a superlattice structure (SL) of carbon spikes in Si. Similarly to the extensively used boron doping SLs,<sup>2,22</sup> the carbon SLs include 6 carbon spikes, 10 nm wide, with a carbon concentration of  $2 \times 10^{20} \text{ cm}^{-3}$ , spaced 100 nm apart, capped with 50 nm silicon, which were epitaxially grown by molecular beam epitaxy (MBE) on float zone {100} Si substrates at 450 °C. Carbon was evaporated in elemental form from a special high-temperature carbon source. Samples were annealed in a tube furnace in Ar (temperature accuracy 10 K). The diffusive behavior of carbon was measured before and after annealing by SIMS.

In the simulations, carbon was assumed to be incorporated fully as substitutional during growth<sup>7</sup> since no carbon agglomeration had been observed experimentally by transmission electron microscopy in the as-grown samples. In Fig. 4, the experimental and simulated carbon profiles for 850 and 900 °C anneals in an inert atmosphere are shown for different annealing times. The thermally generated self-interstitials and vacancies are simulated by injection from the

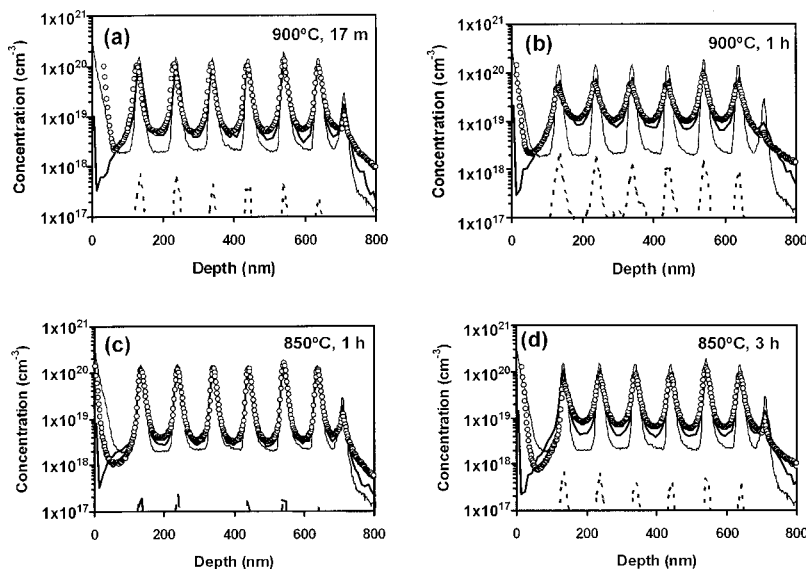


FIG. 4. Experimental (symbols) and simulated (thick solid lines) carbon diffusion profiles for annealings at (a) 900 °C, 17 min; (b) 900 °C, 1 h; (c) 850 °C, 1 h; and (d) 850 °C, 3 h. Dashed lines show the fraction of carbon in clusters containing more than two carbon atoms. The MBE as-grown carbon profile has also been included (thin solid line) as a reference.



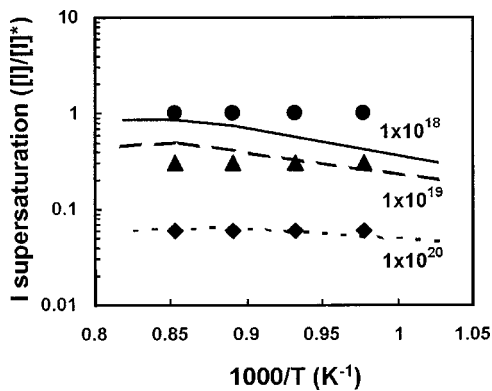


FIG. 5. Self-interstitial supersaturation,  $[I]/[I]^*$ , as a function of temperature for three different carbon concentrations. Symbols are experimental values from Ref. 1, extracted from boron diffusivity experiments for different carbon concentrations: (●)  $10^{18} \text{ cm}^{-3}$ , (▲)  $10^{19} \text{ cm}^{-3}$ , and (◆)  $10^{20} \text{ cm}^{-3}$ . Lines are the corresponding simulated values.

surface. A good fit is observed in all cases. In the simulated profiles, a fraction of carbon immobilized in small C/I clusters with approximately the same content of carbon and self-interstitials appears in every spike, as is shown in Fig. 4. The simulation indicates that at the beginning of the anneal, a high concentration of  $C_2$  clusters is formed. During this initial formation of  $C_2$  clusters, the spread of the carbon spikes in the simulation is much more pronounced than that predicted by the kick-out model alone, in agreement with the experiments of several authors.<sup>1,7</sup> This effect was already shown to be due to the shorter long-hops<sup>23</sup> of the  $C_i$  in the presence of a high concentration of substitutional carbon, forming  $C_2I$  and finally releasing an I and leaving a  $C_2$ .<sup>14</sup>  $C_2$  clusters would be metastable, in the sense that their potential energy ( $-1.1 \text{ eV}$  in our parameter set) is relatively high, but they cannot break up without the intervention of a point defect because their component atoms ( $C_s$ ) are immobile. The other alternative, the reaction  $C_2 \rightarrow C_2I + V$ , is energetically unfavorable. A pair formed by carbon atoms in adjacent substitutional sites ( $C_s-C_s$ ) has been detected by both IRS<sup>24</sup> and electronic paramagnetic resonance,<sup>24,25</sup> and studied by *ab-initio* calculations.<sup>24,25</sup>

The subsequent formation of bigger C/I clusters during the following steps of annealing is controlled by the concentrations of intrinsic point defects. In the case of an inert atmosphere, the self-interstitial flux in the carbon-rich regions is low and the forward reaction 7 (see Fig. 1) can be favored against forward reaction 6. This would be the case for  $C_nI_m$  clusters whose potential energy is much higher than that of  $C_nI_{m+1}$ . This would lead to the growth of the clusters and the generation of vacancies. Since the flux of  $C_i$  is also high under conditions of high carbon concentration, these clusters can also grow by capturing a  $C_i$  (forward reaction 5). Therefore, the growth of  $C_nI_m$  clusters will follow the path indicated in Fig. 1, capturing and emitting the particles that are shown there. These clusters could be the embryos of small SiC precipitates, as it was suggested for  $As_nV_m$  clusters and As precipitates in Ref. 26.

## Self-interstitial undersaturation and vacancy supersaturation in carbon-rich samples

To further test the model, we carried out simulations of a uniform background of carbon at different temperatures, ranging from 700 to 950 °C in an inert atmosphere. The simulated time-averaged supersaturation of self-interstitials ( $[I]/[I]^*$ ) are shown in Fig. 5, where they can be compared with experiments that measure the I supersaturation using boron spikes.<sup>1</sup> Good agreement is obtained for different carbon concentrations. Contrary to the predictions of the simple kick-out model and in agreement to the experiments,<sup>1</sup> the simulated results exhibit a weak dependence of  $[I]/[I]^*$  on temperature. Finally, it is noteworthy to point out that a V supersaturation of around two to three is predicted for a carbon concentration of  $1 \times 10^{20} \text{ cm}^{-3}$  in this range of temperatures, also due to the C/I clustering. An experimental V supersaturation of about eight has been inferred from Sb diffusion in carbon-rich samples.<sup>8</sup>

## CONCLUSIONS

In this work, we have developed a comprehensive model for carbon diffusion and clustering in silicon. The model describes well the observed low temperature pairing of carbon, explains quantitatively the carbon diffusion profiles at 850 and 900 °C and reconciles the experimental V supersaturation measured in this temperature range with a high V formation energy. In addition, the model provides self-interstitial concentration values in agreement with measurements for different temperatures and carbon concentrations. In summary, the model includes several simultaneous mechanisms that allow it to yield correct predictions under a wide variety of experimental conditions.

## ACKNOWLEDGMENT

The authors are grateful to P. Werner for helpful discussions and experimental data.

- <sup>1</sup>H. Rücker, B. Heinemann, W. Röpke, R. Kurps, D. Krüger, G. Lippert, and H. J. Osten, *Appl. Phys. Lett.* **73**, 1682 (1998).
- <sup>2</sup>P. A. Stolk, H.-J. Gossmann, D. J. Eaglesham, D. C. Jacobson, C. S. Rafferty, G. H. Gilmer, M. Jaraiz, J. M. Poate, H. S. Luftman, and T. E. Haynes, *J. Appl. Phys.* **81**, 6031 (1997).
- <sup>3</sup>U. Gösele, *Mater. Res. Soc. Symp. Proc.* **59**, 419 (1986).
- <sup>4</sup>H. Bracht, E. E. Haller, and R. Clark-Phelps, *Phys. Rev. Lett.* **81**, 393 (1998).
- <sup>5</sup>A. R. Bean and R. C. Newman, *J. Phys. Chem. Solids* **32**, 1211 (1971).
- <sup>6</sup>F. Rollert, N. A. Stolwijk, and H. Mehrer, *Mater. Sci. Forum* **38–41**, 753 (1989).
- <sup>7</sup>P. Werner, H.-J. Gossmann, D. C. Jacobson, and U. Gösele, *Appl. Phys. Lett.* **73**, 2465 (1998).
- <sup>8</sup>H. Rücker, B. Heinemann, D. Bolze, D. Knoll, D. Krüger, R. Kurps, H. J. Osten, P. Schley, B. Tillack, and P. Zaumseil, *Tech. Dig. Int. Electron Devices Meet.* **1999**, 345.
- <sup>9</sup>G. D. Watkins, in *Radiation Effects in Semiconductors*, edited by M. Hulin (Dunod, Paris 1965).
- <sup>10</sup>R. F. Scholz, P. Werner, U. Gösele, and T. Y. Tan, *Appl. Phys. Lett.* **74**, 392 (1999).
- <sup>11</sup>See, for example, H. Bracht, N. A. Stolwijk, and Mehrer, *Phys. Rev. B* **52**, 16 542 (1995), and references therein.
- <sup>12</sup>R. A. Casali, H. Rücker, and M. Methfessel, *Appl. Phys. Lett.* **78**, 913 (2001).
- <sup>13</sup>P. E. Blöchl, E. Smargiassi, R. Car, D. B. Laks, W. Andreoni, and S. T. Pantelides, *Phys. Rev. Lett.* **70**, 2435 (1993).

- <sup>14</sup>R. Pinacho, M. Jaraiz, H.-J. Gossmann, G. H. Gilmer, J. L. Benton, and P. Werner, *Mater. Res. Soc. Symp. Proc.* **610**, B7.2 (2000).
- <sup>15</sup>M. Jaraiz, P. Castrillo, R. Pinacho, L. Pelaz, J. Barbolla, G.-H. Gilmer, and C. S. Rafferty, *Mater. Res. Soc. Symp. Proc.* **610**, B11.1 (2000).
- <sup>16</sup>L. W. Song and G. D. Watkins, *Phys. Rev. B* **42**, 5759 (1990).
- <sup>17</sup>S. Coffa and S. Libertino, *Appl. Phys. Lett.* **73**, 3369 (1998).
- <sup>18</sup>J. Zhu, T. Díaz de la Rubia, and C. Mailhot, *Mater. Res. Soc. Symp. Proc.* **439**, 59 (1997).
- <sup>19</sup>E. V. Lavrov, L. Hoffmann, and B. Bech Nielsen, *Phys. Rev. B* **60**, 8081 (1999).
- <sup>20</sup>L. Pelaz, G. H. Gilmer, H. J. Gossmann, C. S. Rafferty, M. Jaraiz, and J. Barbolla, *Appl. Phys. Lett.* **74**, 3657 (1999).
- <sup>21</sup>U. Gösele, P. Laveant, R. Scholz, N. Engler, and P. Werner, *Mater. Res. Soc. Symp. Proc.* **610**, B7.1 (2000).
- <sup>22</sup>H.-J. Gossmann, P. A. Stolk, D. J. Eaglesham, G. H. Gilmer, J. M. Poate, *Proc.-Electrochem. Soc.* **64**, 46 (1996).
- <sup>23</sup>The term “long-hop” denote here the distance traveled by a carbon atom as a particular  $C_i$ . See Cowern *et al.*, *Phys. Rev. Lett.* **65**, 2434 (1990) for the case of boron.
- <sup>24</sup>E. V. Lavrov, B. Bech Nielsen, J. R. Byberg, B. Hourahine, R. Jones, S. Öberg, and P. R. Briddon, *Phys. Rev. B* **62**, 158 (2000).
- <sup>25</sup>J. R. Byberg, B. Bech Nielsen, M. Fancuilli, S. K. Estreicher, and P. A. Fedders, *Phys. Rev. B* **61**, 12 939 (2000).
- <sup>26</sup>P. M. Fahey, P. B. Griffin, and J. D. Plummer, *Rev. Mod. Phys.* **61**, 289 (1989).